Commun Nonlinear Sci Numer Simulat 138 (2024) 108222

Contents lists available at ScienceDirect

Communications in Nonlinear Science and Numerical Simulation

journal homepage: www.elsevier.com/locate/cnsns

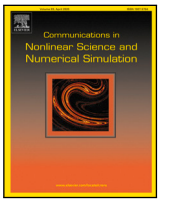

Research paper

Distributed adaptive fault-tolerant control with prescribed performance for nonlinear multiagent systems☆

Li-Ting Lu [a], Shan-Liang Zhu [a,b,c], Dong-Mei Wang [a], Yu-Qun Han [a,b,c,*]

[a] School of Mathematics and Physics, Qingdao University of Science and Technology, Qingdao, 266061, China
[b] Qingdao Innovation Center of Artificial Intelligence Ocean Technology, Qingdao, 266061, China
[c] The Research Institute for Mathematics and Interdisciplinary Sciences, Qingdao University of Science and Technology, Qingdao, 266061, China

ARTICLE INFO

Keywords:
Actuator failures
Prescribed performance control
Distributed adaptive control
Multi-agent systems
Multi-dimensional Taylor network

ABSTRACT

This paper introduces a distributed adaptive fault-tolerant control scheme for nonlinear multi-agent systems afflicted by actuator failures. The proposed scheme ensures that the consensus-tracking errors of the systems meet the prescribed performance requirements. First, in the backstepping design process, a barrier function is constructed based on the proposed scalar function and normalization function to address the prescribed performance issue. Next, both multi-dimensional Taylor network (MTN) control and robust control techniques are utilized to address unknown nonlinear functions. Continuous switching functions are devised to transition from MTN control to robust control whenever the arguments of the unknown functions surpass the operating range of MTN. This effectively resolves the global problem of the system. Furthermore, a boundary estimation method is proposed to handle actuator failures that may occur infinitely. Stability analysis confirms that all signals in the closed-loop system are globally uniformly ultimately bounded. Additionally, the consensus-tracking errors can always be constrained within prescribed boundaries, achieving global convergence to a prescribed accuracy within a prescribed time. Users can flexibly and independently choose the desired settling time and accuracy, without being restricted by any initial conditions. Simulation results provide evidence of the efficacy of the proposed control method.

1. Introduction

With the development of industrial and military applications, cooperative completion of tasks by multiple agents has become increasingly common. As a result, multi-agent cooperative control has garnered significant attention, addressing issues such as consensus problems [1–4], clustering problems [5], formation problems [6], and more. Among them, the leader-following consensus is a fundamental issue of cooperative control. It aims to design a consensus tracking control strategy that enables follower agents to track the trajectory of the leader using information from themselves and neighboring agents. Notable results have been achieved in consensus tracking control for first-order systems [7], second-order systems [8], and high-order systems [9–11]. However, the aforementioned control methods were applicable only to linear multi-agent systems (MASs) or NMASs with known nonlinear functions. When the system contains unknown nonlinear functions, these methods may not be applicable.

In order to address the above issue, numerous intelligent control schemes based on neural networks [12–14], fuzzy logic systems [15–17], and multi-dimensional Taylor network (MTN) [18–20] have been presented. However, research on MTN control

☆ This work was supported by the Shandong Provincial Natural Science Foundation, China (No. ZR2020QF055).

* Corresponding author at: School of Mathematics and Physics, Qingdao University of Science and Technology, Qingdao, 266061, China.
E-mail address: yuqunhan@163.com (Y.-Q. Han).

https://doi.org/10.1016/j.cnsns.2024.108222
Received 28 November 2023; Received in revised form 28 May 2024; Accepted 9 July 2024
Available online 15 July 2024

has not expanded into the realm of NMASs thus far. Moreover, in practical operation, each agent's actuators may encounter unknown failures, resulting in performance degradation and even posing a risk of severe accidents. To eliminate the impact of actuator failures in MASs, fault-tolerant control (FTC) provides an effective solution that ensures system good performance when failures occur. Various FTC methods have been devised, such as the sliding mode FTC method [21], the H_∞ FTC method [22], and the adaptive FTC method [23]. However, it is important to note that the aforementioned FTC methods consider only a limited number of actuator failures per agent and cannot handle an infinite number of failures. In actual factory settings, it is more common for each actuator to experience multiple times failures. To address this issue, the authors in [24] addressed the FTC problem of nonlinear systems with an infinite number of actuator failures for the first time. Inspired by the work of [24], a series of FTC methods [25–28] have been proposed to address the consensus tracking control problem of NMASs with an infinite number of actuator failures. However, it is important to acknowledge that the FTC schemes mentioned earlier offer semi-global stability for the systems, but fall short of achieving global stability.

In recent times, several noteworthy neural control strategies have emerged to attain global stability of the nonlinear systems. Notably, the authors in [29–33] proposed a method in which robust control is employed as a substitute for neural network control when the inputs of a function exceed the active range of the neural network. By leveraging robust control, the system can effectively steer escaping transients back into the active region of the neural network, thereby ensuring global stability. Nonetheless, the investigation into these findings is currently confined to nonlinear systems, neglecting consideration for NMASs. Additionally, the authors in [29,30] achieved the tracking error that satisfies predefined accuracy but falls short of attaining the prescribed accuracy within the specified settling time, significantly limiting its applicability. Meanwhile, the authors in [33] achieved the predetermined time to reach the predefined accuracy, but the transient performance before system steadiness remains unexplored. In addressing these challenges, this paper draws inspiration from [34] and employs a prescribed performance boundary control (PPBC) approach, a technique widely applied to NMASs [35–37]. The PPBC approach employs an error transformation technique and introduces a performance function. By adjusting the performance function, it enables the tracking error to meet the prescribed transient and steady-state performance criteria, including overshoot, convergence rate, and steady-state error. Nevertheless, the aforementioned PPBC methods necessitate suitable initial state values for executing the control strategy. In the event of a system restart or changes in the desired signal, the control strategy requires appropriate adjustments, indicating a dependence on the system's initial conditions. To overcome this limitation, the authors in [38] proposed a novel PPBC method for nonlinear systems that can alleviate the constraints imposed by initial conditions. However, it lacks the flexibility to arbitrarily design the settling time of the systems. Although [39] successfully ensured that the consensus-tracking errors meet prescribed accuracy within a prescribed time, it neglects global system issues and fails to consider problems related to actuator failures. Therefore, achieving the consensus-tracking errors that always vary within a specified range in NMASs with actuator failures, while ensuring global convergence to a prescribed accuracy within a prescribed time, remains a major challenge.

Based on the above discussion, this paper proposes a novel distributed adaptive FTC scheme that can confine the consensus-tracking errors of NMASs with actuator failures within a specified range, while ensuring global convergence to a prescribed accuracy within a prescribed time. Compared to existing methods, this paper offers the following three innovations:

(1) Firstly, different from traditional finite-time and fixed-time control methods [40–42], the proposed scheme in this paper offers a distinctive advantage. It not only ensures a deterministic settling time but also allows for the flexible design of the settling time based on specific requirements. By utilizing this scheme, the consensus-tracking errors are confined within a specified range and achieve convergence to a prescribed accuracy within a prescribed time frame, regardless of the initial conditions of the system.
(2) Secondly, due to the fact that the approximation region of neural networks is a subset of the entire state space, the results provided in [25–28] can only achieve semi-global stability of the system. However, in this paper, a novel approach is introduced where robust control is employed instead of MTN control when the function's inputs exceed the active region of the MTN. This method effectively addresses the challenge of achieving global tracking in NMASs by redirecting escaping transients back into the active region of the MTN.
(3) Finally, this paper also considers the possibility of each actuator in each agent of NMASs experiencing an infinite number of failures. Additionally, by using a finite-time differentiator to approximate the derivative of the virtual control law, rather than directly employing it in the recursive design, the problem of "complexity explosion" is successfully avoided.

2. Problem formulation and preliminaries

2.1. Graph theory

This paper uses graph theory to describe the communication topology between intelligent agents. The directed graph between the agents is denoted as $\zeta = (\mathcal{V}, \mathcal{C}, \mathcal{A})$. The adjacency matrix $\mathcal{A} = [a_{i,j}] \in R^{N\times N}$ describes the connections between nodes. $\mathcal{V} = (1, 2, \dots, N)$ represents the set of nodes, which correspond to the N agents. $\mathcal{C} \subseteq \mathcal{V} \times \mathcal{V}$ is the set of edges between nodes. The set of neighboring nodes of agent i is defined as $\mathcal{N}_i = \{\mathcal{V}_j | (\mathcal{V}_j, \mathcal{V}_i) \in \mathcal{C}, i \neq j\}$. The degree of node i is defined as $d_i = \sum_{j\in\mathcal{N}_i} a_{i,j}$, and the diagonal matrix $\mathcal{D} = \text{diag}\{d_1, d_2, \dots, d_N\}$ is constructed from the degrees of the nodes. The Laplacian matrix of the directed graph ζ is given by $\mathcal{L} = \mathcal{D} - \mathcal{A}$. To expand the graph, we introduce a leader node denoted as 0, and define the expanded graph $\bar{\zeta} = (\bar{\mathcal{V}}, \bar{\mathcal{C}})$, where $\bar{\mathcal{V}} = (0, 1, 2, \dots, N)$ represents the set of nodes, and $\bar{\mathcal{C}} \subseteq \bar{\mathcal{V}} \times \bar{\mathcal{V}}$ is the set of edges between nodes. If node i can receive signals from the leader node 0, then $a_{i,0} > 0$, otherwise $a_{i,0} = 0$. This way, we can model the communication between the agents and the leader node, and analyze the properties of the resulting network.

Lemma 1 ([28]). *If there exists a path that can reach all other nodes from the root node, then the directed graph ζ has a spanning tree. Define $\mathcal{B} = \mathrm{diag}\{a_{1,0}, \ldots, a_{N,0}\}$, where if node 0 is the root of the spanning tree, then the matrix $\mathcal{L} + \mathcal{B}$ is non-singular.*

2.2. Problem formulation

Consider NMASs with N followers, and the dynamics of the followers can be expressed as

$$\begin{cases} \dot{x}_{i,j} = x_{i,j+1} + h_{i,j}\left(\bar{\boldsymbol{x}}_{i,j}\right) + \Lambda_{i,j}(t) \\ \dot{x}_{i,n_i} = \sum_{l=1}^{m_i} b_{i,l} u_{i,l} + h_{i,n_i}\left(\bar{\boldsymbol{x}}_{i,n_i}\right) + \Lambda_{i,n_i}(t) \\ y_i = x_{i,1}, i = 1, \ldots, N, j = 1, \ldots, n_i - 1 \end{cases} \tag{1}$$

where $\bar{\boldsymbol{x}}_{i,j} = \left[x_{i,1}, x_{i,2}, \ldots, x_{i,j}\right]^{\mathrm{T}} \in R^j$ represents the state vector of the followers, while $y_i \in R$ and $u_{i,l} \in R$ denote the output and control input of the followers, respectively. $b_{i,l}$ is an unknown nonzero parameter, and $h_{i,j}\left(\bar{\boldsymbol{x}}_{i,j}\right) : R^j \to R$ is an unknown nonlinear function that satisfies $h_{i,j}(\mathbf{0}) = 0$. Additionally, $\Lambda_{i,j}(t)$ represents an unknown external disturbance that satisfies $\left|\Lambda_{i,j}(t)\right| \le \bar{\Lambda}_{i,j}$, where $\bar{\Lambda}_{i,j} > 0$ is an unknown constant. Each follow agent's actuators may experience faults. Drawing inspiration from [25], the actuator fault model can be represented as follows

$$u_{i,l}(t) = \rho_{i,l}^q(t) u_{i,cl}(t) + \bar{u}_{i,l}^q(t), \forall t \in \left[t_{i,l}^q, t_{i,l}^{q+1}\right) \tag{2}$$

$$\rho_{i,l}^q(t)\bar{u}_{i,l}^q(t) = 0, i = 1, 2, \ldots, N \tag{3}$$

where $u_{i,cl}(t) \in R$ is the control signal that needs to be designed, $q \in N^+$ represents the number of failures occurring in the lth actuator of the ith agent. The terms $t_{i,l}^q$ and $t_{i,l}^{q+1}$ correspond to the start and end times of the failure, satisfying $0 \le t_{i,l}^q < t_{i,l}^{q+1}$. Additionally, $\rho_{i,l}^q(t) \in [0, 1)$ and $\bar{u}_{i,l}^q(t)$ represent unknown time-varying fault parameters. The Eq. (2) indicates that the lth actuator of the ith agent experiences actuator failures at time $t \in \left[t_{i,l}^q, t_{i,l}^{q+1}\right)$, and Eq. (3) implies the following three situations

(1) $\rho_{i,l}^q(t) \neq 0$ and $\bar{u}_{i,l}^q(t) = 0$, where $0 < \rho_{i,l}^q(t) < 1$. This implies that the actuator experiences partial failure.
(2) $\rho_{i,l}^q(t) = 0$ and $\bar{u}_{i,l}^q(t) \neq 0$, where $\rho_{i,l}^q(t) = 0$ implies that the actuator experiences complete failure. The signal $u_{i,l}(t)$ becomes impervious to the influence of control inputs $u_{i,cl}(t)$, and the closed-loop system becomes exclusively influenced by $\bar{u}_{i,l}^q(t)$. Consequently, $u_{i,l}(t)$ is stuck by an unknown bounded signal $\bar{u}_{i,l}^q(t)$.
(3) $\rho_{i,l}^q(t) = 0$ and $\bar{u}_{i,l}^q(t) = 0$. This scenario corresponds to the Float type of complete failures as described in [43].

Remark 1. From (3), it is evident that $\rho_{i,l}^q(t)$ and $\bar{u}_{i,l}^q(t)$ cannot both be greater than zero simultaneously. Therefore, the fault model considered in this paper does not include bias failures, *i.e.*, $u_{i,l}(t) = u_{i,cl} + \bar{u}_{i,l}^q(t)$. Compared to the fault model that includes bias faults as discussed in [44], the fault model in this paper features time-varying parameters, indicating that each actuator can experience an infinite number of failures.

It is worth noting that the description of the communication topology among the agents using the graph ζ, where one agent is designated as the leader. The leader's signal y_d can be generated by the following method

$$\dot{y}_d = \varphi\left(y_d, t\right) \tag{4}$$

where φ is a known function, and the synchronization error of the follower agent i is

$$e_i = \sum_{r=1}^{N} a_{i,r}\left(y_i - y_r\right) + a_{i,0}\left(y_i - y_d\right) \tag{5}$$

where $a_{i,r} \ge 0$ refers to the elements of the adjacency matrix $\mathcal{A}$. If the agent i is unable to receive information from the agent r, then $a_{i,r} = 0$. Similarly, $a_{i,0} \ge 0$ represents the weight of the edge from the leader to the follower agent i. If the follower agent i cannot receive information from the leader, then $a_{i,0} = 0$.

The control objectives of this paper is to develop a distributed adaptive FTC scheme for NMASs (1) with actuator failures, such that: (i) all states of NMASs (1) are globally uniformly ultimately bounded (GUUB); (ii) the consensus-tracking errors e_i is always limited within a specified boundary; (iii) the consensus-tracking errors e_i converges to a prescribed accuracy within a prescribed time.

Assumption 1 ([27]). At any given time, at most $m_i - 1$ actuators can experience complete failures.

Assumption 2 ([25]). For $i = 1, 2, \ldots, N$ and $l = 1, 2, \ldots, m_i$, $b_{i,l}$ is an unknown nonzero parameter, and the sign of $b_{i,l}$ is known (*i.e.*, $\mathrm{sgn}(b_{i,l})$ is known).

Assumption 3 ([25]). In the case of partial failure, the fault parameter $\rho_{i,l}^{q}(t)$ has an unknown constant $\underline{\rho}_{i,l}$ such that $0 \leq \underline{\rho}_{i,l} \leq \rho_{i,l}^{q}(t) < 1$. In the case of complete failure, the fault parameter $\bar{u}_{i,l}^{q}(t)$ has an unknown constant $\bar{\bar{u}}_{i,l} > 0$ such that $\left|\bar{u}_{i,l}^{q}(t)\right| \leq \bar{\bar{u}}_{i,l}^{q}$, where $i = 1, 2, \ldots, N$, $l = 1, 2, \ldots, m_i$.

Assumption 4 ([33]). The nonlinear function $h_{i,j}(\bar{\boldsymbol{x}}_{i,j})$ in the system (1) is bounded, and there exists a constant $d_{i,j}^{f} > 0$ such that $\left|h_{i,j}(\bar{\boldsymbol{x}}_{i,j})\right| \leq d_{i,j}^{f}$.

Assumption 5 ([28]). The directed graph ζ has a spanning tree. The desired trajectory y_d of node 0 is a virtual leader, which is known and demonstrates at least twice continuous differentiability while remaining bounded.

Remark 2. Assumption 1 is common in the existing literatures [25,27] to ensure controllability. It is important to note that as long as at least one actuator is not in a completely failed state, the actuators can experience both partial and complete failures simultaneously. Assumptions 2–3 form the basic requirements for adaptive backstepping control and FTC schemes, as confirmed by numerous studies [25,26]. To ensure safe and stable operation in practice, it is required that the system's state operates within permissible limits. Therefore, the nonlinear functions controlling the state dynamics should be bounded, making Assumption 4 necessary and acceptable. In practical engineering applications, the leader's output y_d can be accurately characterized by differential equations and bounded functions. Thus, Assumption 5 is reasonable and can be found in [28].

Lemma 2 ([20]). *Given a bounded closed set $\Omega \subset R^n$ and a continuous function $F(\chi) : R^n \to R$, with $\varepsilon > 0$ as a given constant, we can establish the existence of an MTN that fulfills the following conditions*

$$F(\chi) = \boldsymbol{W}^{*\mathrm{T}} S_{m_n}(\chi) + \delta(\chi), \ |\delta(\chi)| \leq \varepsilon \tag{6}$$

where $\chi = [\chi_1, \chi_2, \ldots, \chi_n] \in \Omega$ denotes the input vector of the MTN, $\boldsymbol{W}^* = \left[W_1^*, W_2^*, \ldots, W_l^*\right]^{\mathrm{T}} \in R^l$ represents the weight vector of the MTN, and $S_{m_n}(\chi) = [\chi_1, \ldots, \chi_n, \chi_1^2, \chi_1\chi_2, \ldots, \chi_n^2, \chi_1^m, \chi_1^{m-1}\chi_2, \ldots, \chi_n^m]^{\mathrm{T}} \in R^l$ stands for the middle layer vector of the MTN. The function $\delta(\chi)$ represents the approximation error, and it satisfies the condition $|\delta(\chi)| \leq \varepsilon$, where ε is a positive constant.

Remark 3. Neural networks control [44] and fuzzy logic systems control [45,46] are commonly employed to approximate complex and uncertain nonlinear functions within systems. MTN, resembling radial basis function neural networks (RBFNNs), comprises three layers: input, middle, and output layers. Diverging from RBFNNs, MTN's middle layer substitutes polynomials for radial basis functions. In essence, MTN can be viewed as an RBFNNs with a distinctive structure.

2.3. Key definitions

Consider the following non-autonomous system

$$\dot{\boldsymbol{x}} = g(\boldsymbol{x}(t)), \quad \boldsymbol{x}(t_0) = \boldsymbol{x}_0 \tag{7}$$

where $g : R^n \times [t_0, \infty) \to R^n$ is a continuous vector function. $\boldsymbol{x}(t) \in R^n$ is a solution to (7) and $\boldsymbol{x}_0 \in R^n$ represents the value of $\boldsymbol{x}(t)$ at time t_0, where $t_0 \in [0, \infty)$.

Definition 1 ([47]). Considering system (7), if there exists a compact set $U \subset R^n$, for every $\boldsymbol{x}_0 \in U$, there exist a constant $\varrho > 0$ and a time $T(\varrho, \boldsymbol{x}_0)$ satisfying $\|\boldsymbol{x}(t)\| \leq \varrho$ for all $t \geq t_0 + T(\varrho, \boldsymbol{x}_0)$, we classify the solutions of system (7) as semi-globally uniformly ultimately bounded (SGUUB). Specifically, if $U = R^n$, we categorize the solutions of system (7) as GUUB.

Definition 2 ([39]). Suppose there exists a function $\phi_i(t)$ that satisfies the following two conditions: (i) $\phi_i(t)$ is at least twice continuously differentiable. (ii) The function $\phi_i(t)$ increases from an initial value of $\phi_i(0) = 1$ to a final value of $\phi_i(T_s) = \frac{1}{\gamma_i}$, where $0 < \gamma_i < 1$ is a design parameter, and $T_s > 0$ is a settling time that can be arbitrarily chosen. Once $t \geq T_s$, $\phi_i(t) = \frac{1}{\gamma_i}$. Then, $\phi_i(t)$ can serve as a performance scalar function defined over the interval $[0, \infty)$.

Definition 3 ([33]). Define the following switching function

$$k(\upsilon) = \begin{cases} 1, & |\upsilon| \leq \iota_1 \\ \cos^n\left[\frac{\pi}{2}\sin^n\left(\frac{\pi}{2}\frac{|\upsilon|^2 - \iota_1^2}{\iota_2^2 - \iota_1^2}\right)\right], & \text{otherwise} \\ 0, & |\upsilon| \geq \iota_2 \end{cases} \tag{8}$$

where ι_1 and ι_2 are constant values satisfying $\iota_2 > \iota_1 > 0$ and serve as the lower and upper bounds, respectively, for the switching variable υ.

Let

$$K(\chi) := \prod_{i=1}^{m} k(\upsilon_i) \tag{9}$$

where $\chi = [\upsilon_1, \upsilon_2, \ldots, \upsilon_m]^{\mathrm{T}} \in R^m$. This is the key to design a globally stable adaptive MTN controller.

3. Global adaptive MTN consensus FTC design

3.1. Prescribed performance functions

In this paper, we construct the following prescribed performance function

$$\psi_i(\emptyset_i) = \frac{\sqrt{\eta_i}\emptyset_i}{\sqrt{1-\emptyset_i^2}} \tag{10}$$

where $\eta_i > 0$ is a design parameter, $\emptyset_i(t) = \frac{1}{\phi_i(t)}$ with $\phi_i(t)$ is a scalar function satisfies Definition 2. The scalar function $\phi_i(t)$ is defined as follows

$$\phi_i(t) = \begin{cases} \frac{1}{(1-\gamma_i)(\frac{T_s-t}{T_s})^3 \exp(-\check{k}t)+\gamma_i}, & t < T_s \\ \frac{1}{\gamma_i}, & t \geq T_s \end{cases} \tag{11}$$

where $\check{k} > 0$ is a design parameter.

Remark 4. Clearly, the successful realization of the second and third control objectives critically depends on satisfying the condition $-\psi_i(\emptyset_i) < e_i < \psi_i(\emptyset_i)$. This is because, at $t = 0$, the range of e_i spans from $(-\infty, \infty)$; for $t \in (0, T_s)$, the range narrows to $\left(-\frac{\sqrt{\eta_i}}{\sqrt{\phi_i^2-1}}, \frac{\sqrt{\eta_i}}{\sqrt{\phi_i^2-1}}\right)$; and for $t \geq T_s$, it further refines to $\left(-\frac{\sqrt{\eta_i}\gamma_i}{\sqrt{1-\gamma_i^2}}, \frac{\sqrt{\eta_i}\gamma_i}{\sqrt{1-\gamma_i^2}}\right)$. Therefore, by successfully designing a controller that maintains the condition $\psi_i(-\emptyset_i(t)) < e_i < \psi_i(\emptyset_i(t))$, we can effectively achieve the second and third control objectives.

Remark 5. Diverging from traditional finite-time and fixed-time control approaches [40–42], this paper allows the settling time T_s to be arbitrarily designed by users, without the need to consider initial conditions. Additionally, the transient performance of synchronization errors e_i before reaching steady state is guaranteed. Both the transient performance boundary $\frac{\sqrt{\eta_i}}{\sqrt{\phi_i^2-1}}$ and the steady-state performance boundary $\frac{\sqrt{\eta_i}\gamma_i}{\sqrt{1-\gamma_i^2}}$ can be tailored to user preferences, independent of initial conditions.

Furthermore, to achieve the first control objective, and eliminate the constraints on the initial conditions of the tracking error, a normalization function is proposed as follows

$$\Psi_i(e_i) = \frac{e_i}{\sqrt{e_i^2+\eta_i}} \tag{12}$$

where $\Psi_i(e_i)$ is the inverse function of $\psi_i(\cdot)$. Clearly, $\Psi_i(e_i)$ adheres to the following features:

(i) $\Psi_i(e_i)$ is strictly monotonical;
(ii) $\Psi_i(e_i) \in (-1, 1)$ always holds for any $e_i \in R$;
(iii) $\lim_{e_i \to \infty} \Psi_i(e_i) = 1$ and $\lim_{e_i \to -\infty} \Psi_i(e_i) = -1$;
(iv) $e_i = 0 \Longleftrightarrow \Psi_i(e_i) = 0$.

Remark 6. According to Remark 4, if the condition $-\psi_i(\emptyset_i) < e_i < \psi_i(\emptyset_i)$ is satisfied, the second and third control objectives can be achieved. Since $\Psi_i(e_i)$ is the inverse function of $\psi_i(\cdot)$, we have $\psi_i(\Psi_i(e_i)) = e_i$. Consequently, it can be deduced that $-\psi_i(\emptyset_i) < \psi_i(\Psi_i(e_i)) < \psi_i(\emptyset_i)$. Furthermore, due to the monotonically increasing nature of $\psi_i(\cdot)$ within its domain, if the condition $-\emptyset_i < \Psi_i(e_i) < \emptyset_i$ is met, the control objectives can be realized. In this study, a barrier function is designed to easily satisfy this condition. As a result, this transformation effectively eliminates the limitations imposed by the initial conditions of the system.

3.2. Controller design procedures

With the development of adaptive backstepping techniques, a global adaptive FTC scheme based on MTN is proposed in this section to handle the prescribed tracking error performance and actuator failures problem. First of all, a coordinate transformation is defined as follows

$$z_i(t) = \phi_i(t)\Psi_i(e_i). \tag{13}$$

In accordance with the control objectives and inspired by Remark 6, the following barrier function can be constructed as

$$\iota_i = \frac{z_i(t)}{1 - z_i^2(t)} \tag{14}$$

Therefore, the following coordinate transformation is defined as

$$\begin{cases} s_{i,1} = \iota_i \\ s_{i,j} = x_{i,j} - \alpha_{i,j-1}, j = 2, 3, \dots, n_i \end{cases} \tag{15}$$

where $\alpha_{i,j-1}$ represents the virtual control signal, for $i = 1, 2, \dots, N$, and $j = 2, \dots, n_i$.

Remark 7. Based on the properties of $\Psi_i(e_i)$, we have $z_i(0) = \phi_i(0)\Psi_i(e(0)) = \Psi_i(e(0)) \in (-1, 1)$, therefore, $s_{i,1}$ is initially well-defined. Further, it can be seen that $s_{i,1}$ tends to $\pm\infty$ if and only if z_i tends to ±1, *i.e.*, for any $|z_i(0)| < 1$, $s_{i,1} \to \pm\infty$ if and only if $z_i \to +1$ or $z_i \to -1$. This important property of $s_{i,1}$ implies that for any bounded initial tracking error $z_i(0)$, as long as $s_{i,1}$ remains bounded, $z_i(t)$ will naturally always stay within the set $\Omega_{z_i} = \{z_i \in \mathbb{R} \mid |z_i| < 1\}$.

Step 1: According to (13) and (14), we have

$$\dot{s}_{i,1} = \tau_{i,1}\dot{z}_i = \tau_{i,1}\left(\dot{\phi}_i(t)\Psi_i(e_i) + \phi_i(t)\tau_{i,2}\dot{e}_i\right) \tag{16}$$

where $\tau_{i,1} = \frac{z_i^2+1}{(1-z_i^2)^2}$, $\tau_{i,2} = \frac{\eta_i}{\sqrt{e_i^2+\eta_i}(e_i^2+\eta_i)}$.

Selecting the first Lyapunov function as follows

$$V_{i,1} = \frac{1}{2}s_{i,1}^2 + \frac{1}{2}\tilde{\hbar}_{i,1}^2 + \frac{1}{2}\tilde{\vartheta}_{i,1}^2 \tag{17}$$

where $\tilde{\hbar}_{i,1} = \hbar_{i,1} - \hat{\hbar}_{i,1}$ represents the parameter error, with $\hat{\hbar}_{i,1}$ being the estimate of $\hbar_{i,1}$, and $\hbar_{i,1}$ will be defined in (20). Similarly, $\tilde{\vartheta}_{i,1} = \vartheta_{i,1} - \hat{\vartheta}_{i,1}$ represents the parameter error, with $\hat{\vartheta}_{i,1}$ being the estimate of $\vartheta_{i,1}$, and $\vartheta_{i,1}$ will be defined in (21).

Subsequently, using (17) together with (1), (5) and (16), we can derive the result as

$$\begin{aligned} \dot{V}_{i,1} = {} & s_{i,1}\left(M_{i,1} + N_{i,1}\left(s_{i,2} + \alpha_{i,1} + \Lambda_{i,1}\right) - N_{i,1}A_i\left(x_{r,2} + \Lambda_{r,1}\right)\right. \\ & \left. + N_{i,1}\left(F_{i,1} - B_i\dot{y}_d\right)\right) - \tilde{\hbar}_{i,1}\dot{\hat{\hbar}}_{i,1} - \tilde{\vartheta}_{i,1}\dot{\hat{\vartheta}}_{i,1} \end{aligned} \tag{18}$$

where $A_i = \frac{\sum_{r=1}^{N} a_{i,r}}{\sum_{r=1}^{N} a_{i,r}+a_{i,0}}$, and $B_i = \frac{a_{i,0}}{\sum_{r=1}^{N} a_{i,r}+a_{i,0}}$ $M_{i,1} = \tau_{i,1}\dot{\phi}_i(t)\Psi_i(e_i)$, $N_{i,1} = \tau_{i,1}\tau_{i,2}\phi_i(t)\left(\sum_{r=1}^{N} a_{i,r} + a_{i,0}\right)$, $F_{i,1} = h_{i,1} - A_i h_{r,1}$.

Indeed, the direct use of unknown functions $h_{i,1}$ and $h_{r,1}$ for controller design is not viable. Thus, following Lemma 2, the MTN can be employed to approximate the unknown function $F_{i,1}$ as $F_{i,1} = \boldsymbol{W}_{i,1}^{\mathrm{T}} S_{m_{i,1}} + \delta_{i,1}$, with $|\delta_{i,1}| \le \varepsilon_{i,1}$ representing the approximation error. Next, based on $\left|\Lambda_{i,j}(t)\right| \le \bar{\Lambda}_{i,j}$, let $\bar{\boldsymbol{W}}_{i,1} = \left[\boldsymbol{W}_{i,1}^{\mathrm{T}}, \varepsilon_{i,1}, \bar{\Lambda}_{i,1}, \bar{\Lambda}_{r,1}\right]^{\mathrm{T}}$ and $\bar{S}_{m_{i,1}} = [S_{m_{i,1}}, 1, 1, 1]^{\mathrm{T}}$. By combining these with the Young's inequality, we can derive the following

$$F_{i,1} + \Lambda_{i,1} - A_i\Lambda_{r,1} \le \bar{\boldsymbol{W}}_{i,1}^{\mathrm{T}}\bar{S}_{m_{i,1}} \tag{19}$$

$$N_{i,1}s_{i,1}\left(F_{i,1} + \Lambda_{i,1} - A_i\Lambda_{r,1}\right) \le \left(\frac{1}{2} + \frac{1}{2}N_{i,1}^2\hbar_{i,1}\bar{S}_{m_{i,1}}^{\mathrm{T}}\bar{S}_{m_{i,1}}\right)|s_{i,1}| \tag{20}$$

where $\hbar_{i,1} = \|\bar{\boldsymbol{W}}_{i,1}\|^2$.

Remark 8. According to Lemma 2, for the MTN to approximate unknown functions, it is essential that the input layer remains within the compact set Ω. Given this constraint, achieving global stability for the system presents significant challenges. Therefore, different from [25–28], this paper introduces the switching function as defined in Definition 3. When the parameters of the unknown function surpass the working range of the MTN, the system switches to robust control, effectively meeting global performance requirements.

Nevertheless, when the parameters of the unknown function $F_{i,1}$ surpass the operating range of the MTN, robust control is implemented to handle $F_{i,1}$. By Assumption 4, we obtain

$$F_{i,1} + \Lambda_{i,1} - A_i\Lambda_{r,1} \le d_{i,1}^f + d_{r,1}^f + \bar{\Lambda}_{i,1} + \bar{\Lambda}_{r,1} \triangleq \vartheta_{i,1} \tag{21}$$

$$N_{i,1}s_{i,1}\left(F_{i,1} + \Lambda_{i,1} - A_i\Lambda_{r,1}\right) \le N_{i,1}|s_{i,1}|\vartheta_{i,1} \tag{22}$$

Naturally, the feasible virtual control signal $\alpha_{i,1}$ can be designed as follows

$$\begin{aligned} \alpha_{i,1} = {} & -\frac{c_{i,1}s_{i,1}}{N_{i,1}} - \hat{\vartheta}_{i,1}\mathrm{sign}(s_{i,1})\left(1 - K(\chi_{i,1})\right) \\ & - \left(\frac{1}{2N_{i,1}} + \frac{1}{2}N_{i,1}\hat{\hbar}_{i,1}\bar{S}_{m_{i,1}}^{\mathrm{T}}\bar{S}_{m_{i,1}}\right)\mathrm{sign}(s_{i,1})K(\chi_{i,1}) \\ & + B_i\dot{y}_d + A_i x_{r,2} - \frac{M_{i,1}}{N_{i,1}} \end{aligned} \tag{23}$$

The parameter adaptive laws $\dot{\hat{\hbar}}_{i,1}$ and $\dot{\hat{\vartheta}}_{i,1}$ are given as follows

$$\dot{\hat{\hbar}}_{i,1} = \left(\frac{1}{2}|s_{i,1}|N_{i,1}^2\bar{S}_{m_{i,1}}^{\mathrm{T}}\bar{S}_{m_{i,1}} - \hat{\hbar}_{i,1}\right)K(\chi_{i,1}) \tag{24}$$

$$\dot{\hat{\vartheta}}_{i,1} = \left(N_{i,1}|s_{i,1}| - \hat{\vartheta}_{i,1}\right)\left(1 - K(\chi_{i,1})\right) \tag{25}$$

where $c_{i,1} > 0$ is a design parameter, and $\chi_{i,1} = [x_{i,1}, x_{r,1}]^{\mathrm{T}}$.

Subsequently, substituting (20), (22), (23), (24), and (25) into (18), we obtain

$$\dot{V}_{i,1} \le -c_{i,1}s_{i,1}^2 + \left|\tilde{\hbar}_{i,1}\hat{\hbar}_{i,1}\right| + \left|\tilde{\vartheta}_{i,1}\hat{\vartheta}_{i,1}\right| + N_{i,1}s_{i,1}s_{i,2} \tag{26}$$

Step j $(2 \le j \le n_i - 1)$: For the purpose of estimating $\dot{\alpha}_{i,j-1}$, a finite-time differentiator is specifically introduced as

$$\begin{cases} \dot{\varpi}_{i,j-1} = \breve{\varpi}_{i,j-1} - \breve{a}_i \mathrm{sig}\left(p_{i,j-1}\right)^{\frac{1}{2}} \\ \dot{\breve{\varpi}}_{i,j-1} = -\breve{b}_i \mathrm{sign}\left(p_{i,j-1}\right) \end{cases} \tag{27}$$

where $p_{i,j-1} = \varpi_{i,j-1} - \alpha_{i,j-1}$, $\varpi_{i,j-1}$ and $\breve{\varpi}_{i,j-1}$ are the states of the differentiator, $\breve{a}_i$ and $\breve{b}_i$ are the differentiator parameters, and $\mathrm{sig}\left(p_{i,j-1}\right)^{\frac{1}{2}} = \left|p_{i,j-1}\right|^{\frac{1}{2}}\mathrm{sign}\left(p_{i,j-1}\right)$. According to [48], as long as the initial deviations $\varpi_{i,j-1}(0) - \alpha_{i,j-1}(0)$ and $\breve{\varpi}_{i,j-1}(0) - \dot{\alpha}_{i,j-1}(0)$ are bounded, the differentiator (27) can provide $\dot{\alpha}_{i,j-1}$ with arbitrary accuracy. Therefore, $\dot{\alpha}_{i,j-1} = \breve{\varpi}_{i,j-1} + \epsilon_{i,j-1}$ holds, and there exists a constant $\bar{\epsilon}_{i,j-1} > 0$ such that $\left|\epsilon_{i,j-1}\right| \le \bar{\epsilon}_{i,j-1}$.

Selecting the jth Lyapunov function as follows

$$V_{i,j} = V_{i,j-1} + \frac{1}{2}s_{i,j}^2 + \frac{1}{2}\tilde{\hbar}_{i,j}^2 + \frac{1}{2}\tilde{\vartheta}_{i,j}^2 \tag{28}$$

where $\tilde{\hbar}_{i,j} = \hbar_{i,j} - \hat{\hbar}_{i,j}$ represents the parameter error, with $\hat{\hbar}_{i,j}$ being the estimate of $\hbar_{i,j}$, and $\hbar_{i,j}$ will be defined in (31). Similarly, $\tilde{\vartheta}_{i,j} = \vartheta_{i,2} - \hat{\vartheta}_{i,j}$ represents the parameter error, with $\hat{\vartheta}_{i,j}$ being the estimate of $\vartheta_{i,j}$, and $\vartheta_{i,j}$ will be defined in (32).

By using (28) and according to (1), the derivative of $V_{i,j}$ is given by

$$\begin{aligned} \dot{V}_{i,j} \le{}& \dot{V}_{i,j-1} + s_{i,j}\left(\breve{\varpi}_{i,j-1} + \alpha_{i,j} + F_{i,j} + \Lambda_{i,j} - \dot{\alpha}_{i,j-1} + s_{i,j+1}\right) \\ & - s_{i,j}\breve{\varpi}_{i,j-1} - \tilde{\hbar}_{i,j}\dot{\hat{\hbar}}_{i,j} - \tilde{\vartheta}_{i,j}\dot{\hat{\vartheta}}_{i,j} \end{aligned} \tag{29}$$

where $F_{i,j} = h_{i,j}$.

Following the same procedure as in step 1, we have $F_{i,j} = \boldsymbol{W}_{i,j}^{\mathrm{T}}S_{m_{i,j}} + \delta_{i,j}$, with $|\delta_{i,j}| \le \varepsilon_{i,j}$. Moreover, based on the finite-time differentiator (27), we can define $\bar{\boldsymbol{W}}_{i,j} = \left[\boldsymbol{W}_{i,j}^{\mathrm{T}}, \epsilon_{i,j}, \bar{\Lambda}_{i,j}, \bar{\epsilon}_{i,j-1}\right]^{\mathrm{T}}$ and $\bar{S}_{m_{i,j}} = \left[S_{m_{i,j}}, 1, 1, 1\right]^{\mathrm{T}}$. By applying the Young's inequality, we obtain

$$F_{i,j} + \Lambda_{i,j} - \dot{\alpha}_{i,j-1} + \breve{\varpi}_{i,j-1} \le \bar{\boldsymbol{W}}_{i,j}^{\mathrm{T}}\bar{S}_{m_{i,j}} \tag{30}$$

$$s_{i,j}\left(F_{i,j} + \Lambda_{i,j} - \dot{\alpha}_{i,j-1} + \breve{\varpi}_{i,j-1}\right) \le |s_{i,j}|\left(\frac{1}{2} + \frac{1}{2}\hbar_{i,j}\bar{S}_{m_{i,j}}^{\mathrm{T}}\bar{S}_{m_{i,j}}\right) \tag{31}$$

where $\hbar_{i,j} = \|\bar{\boldsymbol{W}}_{i,j}\|^2$.

If the arguments $\bar{\boldsymbol{x}}_{i,j}$ in the functions $F_{i,j}$ surpass the active range of the MTN, robust control is implemented to handle $F_{i,j}$. By Assumption 4, we obtain

$$F_{i,j} + \Lambda_{i,j} - \dot{\alpha}_{i,j-1} + \breve{\varpi}_{i,j-1} \le d_{i,j}^f + \bar{\Lambda}_{i,j} + \bar{\epsilon}_{i,j-1} \triangleq \vartheta_{i,j} \tag{32}$$

$$s_{i,j}\left(F_{i,j} + \Lambda_{i,j} - \dot{\alpha}_{i,j-1} + \breve{\varpi}_{i,j-1}\right) \le |s_{i,j}|\vartheta_{i,j} \tag{33}$$

In this step, the feasible virtual control signal $\alpha_{i,j}$ is designed as follows

$$\begin{aligned} \alpha_{i,j} ={}& -c_{i,j}s_{i,j} - \hat{\vartheta}_{i,j}\mathrm{sign}(s_{i,j})\left(1 - K(\chi_{i,j})\right) \\ & - \left(\frac{1}{2} + \frac{1}{2}\hat{\hbar}_{i,j}\bar{S}_{m_{i,j}}^{\mathrm{T}}\bar{S}_{m_{i,j}}\right)\mathrm{sign}(s_{i,j})K(\chi_{i,j}) - \underline{d}_{i,j}s_{i,j-1} + \breve{\varpi}_{i,j-1} \end{aligned} \tag{34}$$

The parameter adaptive laws $\dot{\hat{\hbar}}_{i,j}$ and $\dot{\hat{\vartheta}}_{i,j}$ are designed as follows

$$\dot{\hat{\hbar}}_{i,j} = \left(\frac{1}{2}|s_{i,j}|\bar{S}_{m_{i,j}}^{\mathrm{T}}\bar{S}_{m_{i,j}} - \hat{\hbar}_{i,j}\right)K(\chi_{i,j}) \tag{35}$$

$$\dot{\hat{\vartheta}}_{i,j} = \left(|s_{i,j}| - \hat{\vartheta}_{i,j}\right)\left(1 - K(\chi_{i,j})\right) \tag{36}$$

where $c_{i,j} > 0$ is a design parameter, $\chi_{i,j} = [x_{i,1}, x_{i,2}, \ldots, x_{i,j}]^{\mathrm{T}}$, and for $j = 2$, $\underline{d}_{i,j} = N_{i,1}$, while for $2 < j \le n_i - 1$, $\underline{d}_{i,j} = 1$.

Subsequently, substituting (31), (33), (34), (35), and (36) into (29), we obtain

$$\dot{V}_{i,j} \le -\sum_{\lambda=1}^{2}c_{i,\lambda}s_{i,\lambda}^2 + \sum_{\lambda=1}^{m}\left|\tilde{\hbar}_{i,\lambda}\hat{\hbar}_{i,\lambda}\right| + \sum_{\lambda=1}^{m}\left|\tilde{\vartheta}_{i,\lambda}\hat{\vartheta}_{i,\lambda}\right| + s_{i,j}s_{i,j+1} \tag{37}$$

Remark 9. From the above, it can be seen that the virtual control law $\alpha_{i,j}$ is a continuous function of the system state $\bar{\boldsymbol{x}}_{i,j}$ and the intermediate variables $s_{i,j-1}$, $s_{i,j}$. Since $\bar{\boldsymbol{x}}_{i,j}$, $s_{i,j-1}$ and $s_{i,j}$ are available, the first derivative of $\alpha_{i,j}$, *i.e.*, $\dot{\alpha}_{i,j}$, can be analytically computed. However, as the system dimension increases, the computation of $\dot{\alpha}_{i,j}$ becomes increasingly complex. In the existing literature, the virtual control $\alpha_{i,j}$ includes $\dot{\alpha}_{i,j-1}$, thus introducing computational complexity. In this paper, however, by utilizing a finite-time differentiator, the repeated computation of $\dot{\alpha}_{i,j-1}$ is avoided, thereby reducing the computational complexity.

Step n_i: Similar to the previous step, we employ the following differentiator to estimate $\dot{\alpha}_{i,n_i-1}$

$$\begin{cases} \varpi_{i,n_i-1} = \breve{\varpi}_{i,n_i-1} - \breve{a}_i \mathrm{sig}\left(p_{i,n_i-1}\right)^{\frac{1}{2}} \\ \dot{\breve{\varpi}}_{i,n_i-1} = -\breve{b}_i \mathrm{sign}\left(p_{i,n_i-1}\right) \end{cases} \tag{38}$$

where $p_{i,n_i-1} = \varpi_{i,n_i-1} - \alpha_{i,n_i-1}$, ϖ_{i,n_i-1} and $\breve{\varpi}_{i,n_i-1}$ are the states of the differentiator, $\breve{a}_i$ and $\breve{b}_i$ are the differentiator parameters, and $\mathrm{sig}\left(p_{i,n_i-1}\right)^{\frac{1}{2}} = \left|p_{i,n_i-1}\right|^{\frac{1}{2}} \mathrm{sign}\left(p_{i,n_i-1}\right)$. Similar to the previous step, we can express $\dot{\alpha}_{i,n_i-1}$ as $\dot{\alpha}_{i,n_i-1} = \breve{\varpi}_{i,n_i-1} + \epsilon_{i,n_i-1}$, where ϵ_{i,n_i-1} represents a bounded estimation error. It is worth noting that there exists a constant $\bar{\epsilon}_{i,n_i-1} > 0$ such that $\left|\epsilon_{i,n_i-1}\right| \le \bar{\epsilon}_{i,n_i-1}$.

From Assumption 3, it is obtained that when $t > 0$, we have $\sum_{l=1}^{m_i} |b_{i,l}| \rho_{i,l}^q \ge \min\left\{ |b_{i,1}| \underline{\rho}_{i,1}^q, |b_{i,2}| \underline{\rho}_{i,2}^q, \ldots, |b_{i,l}| \underline{\rho}_{i,l}^q \right\}$, $\inf_{t\ge 0} \sum_{l=1}^{m_i} |b_{i,l}| \rho_{i,l}^q \ge \min\left\{ |b_{i,1}| \underline{\rho}_{i,1}^q, |b_{i,2}| \underline{\rho}_{i,2}^q, \ldots, |b_{i,l}| \underline{\rho}_{i,l}^q \right\}$. Therefore, to compensate for the unknown actuator failures, we define $\pi_i = \inf_{t\ge 0} \sum_{l=1}^{m_i} |b_{i,l}| \rho_{i,l}^q$ and $\omega_i = \frac{1}{\pi_i}$.

Naturally, we select the n_i-th Lyapunov function as follows

$$V_{i,n_i} = V_{i,n_i-1} + \frac{1}{2} s_{i,n_i}^2 + \frac{1}{2} \tilde{\hbar}_{i,n_i}^2 + \frac{1}{2} \tilde{\vartheta}_{i,n_i}^2 + \frac{\pi_i}{2} \tilde{\omega}_i^2 \tag{39}$$

where $\tilde{\omega}_i = \omega_i - \hat{\omega}_i$ is the parameter error, and $\hat{\omega}_i$ is the estimate of ω_i. Additionally, $\tilde{\hbar}_{i,n_i} = \hbar_{i,n_i} - \hat{\hbar}_{i,n_i}$ represents the parameter error, with $\hat{\hbar}_{i,n_i}$ as the estimate of $\hbar_{i,n_i}$, and $\hbar_{i,n_i}$ will be defined in (42). Similarly, $\tilde{\vartheta}_{i,n_i} = \vartheta_{i,n_i} - \hat{\vartheta}_{i,n_i}$ represents the parameter error, with $\hat{\vartheta}_{i,n_i}$ as the estimate of ϑ_{i,n_i}, and ϑ_{i,n_i} will be defined in (43).

Using (39) and according to (1), (2) and Assumption 3, the derivative of V_{i,n_i} is given by

$$\begin{aligned} \dot{V}_{i,n} \le \dot{V}_{i,n-1} + s_{i,n} \Bigg(& \sum_{l=1}^{m_i} b_{i,l} \rho_{i,l}^q(t) u_{i,cl} + \sum_{l=1}^{m_i} b_{i,l} \bar{\bar{u}}_{i,l}^q \\ & + F_{i,n_i} + \Lambda_{i,n} - \dot{\alpha}_{i,n_i-1} + \breve{\varpi}_{i,n_i-1} \Bigg) - \tilde{\hbar}_{i,n} \dot{\hat{\hbar}}_{i,n} \\ & - \tilde{\vartheta}_{i,n} \dot{\hat{\vartheta}}_{i,n} - \pi_i \tilde{\omega}_i \dot{\hat{\omega}}_i - s_{i,n} \breve{\varpi}_{i,n_i-1} \end{aligned} \tag{40}$$

where $F_{i,n_i} = h_{i,n_i}$.

As in the previous steps, we express $F_{i,n_i} = \boldsymbol{W}_{i,n_i}^{\mathrm{T}} S_{m_{i,n_i}} + \delta_{i,n_i}$, with $|\delta_{i,n_i}| \le \varepsilon_{i,n_i}$. Let $\bar{\boldsymbol{W}}_{i,n_i} = \left[\boldsymbol{W}_{i,n_i}^{\mathrm{T}}, \varepsilon_{i,n_i}, \sum_{l=1}^{m_i} b_{i,l} \bar{\bar{u}}_{i,l}^q, \bar{\Lambda}_{i,n_i}, \bar{\epsilon}_{i,n_i-1}\right]^{\mathrm{T}}$ and $\bar{S}_{m_{i,n_i}} = \left[S_{m_{i,n_i}}, 1, 1, 1, 1\right]^{\mathrm{T}}$. By applying the Young's inequality, it is obtained that

$$\begin{aligned} & \sum_{l=1}^{m_i} b_{i,l} \bar{u}_{i,l}^q + F_{i,n_i} + \Lambda_{i,n_i} - \dot{\alpha}_{i,n_i-1} + \breve{\varpi}_{i,n_i-1} \\ & \le \boldsymbol{W}_{i,n_i}^{\mathrm{T}} S_{m_{i,n_i}} + \varepsilon_{i,n_i} + \sum_{l=1}^{m_i} b_{i,l} \bar{\bar{u}}_{i,l}^q + \bar{\Lambda}_{i,n_i-1} \\ & + \bar{\epsilon}_{i,n_i-1} = \bar{\boldsymbol{W}}_{i,n_i}^{\mathrm{T}} \bar{S}_{m_{i,n_i}} \end{aligned} \tag{41}$$

$$\begin{aligned} & s_{i,n_i} \left(\sum_{l=1}^{m_i} b_{i,l} \bar{u}_{i,l}^q + F_{i,n_i} + \Lambda_{i,n_i} - \dot{\alpha}_{i,n_i-1} + \breve{\varpi}_{i,n_i-1} \right) \\ & \le |s_{i,n_i}| \left(\frac{1}{2} + \frac{1}{2} \hbar_{i,n_i} \bar{S}_{m_{i,n_i}}^{\mathrm{T}} \bar{S}_{m_{i,n_i}} \right) \end{aligned} \tag{42}$$

where $\hbar_{i,n_i} = \|\bar{\boldsymbol{W}}_{i,n_i}\|^2$.

If the arguments $\bar{\boldsymbol{x}}_{i,n_i}$ in the functions F_{i,n_i} surpass the active range of the MTN, robust control is implemented to handle F_{i,n_i}. By Assumption 4, we obtain

$$\begin{aligned} & \sum_{l=1}^{m_i} b_{i,l} \bar{u}_{i,l}^q + F_{i,n_i} + \Lambda_{i,n_i} - \dot{\alpha}_{i,n_i-1} + \breve{\varpi}_{i,n_i-1} \\ & \le \sum_{l=1}^{m_i} b_{i,l} \bar{\bar{u}}_{i,l}^q + d_{i,n_i}^f + \bar{\Lambda}_{i,n_i} + \bar{\epsilon}_{i,n_i-1} \triangleq \vartheta_{i,n_i} \end{aligned} \tag{43}$$

$$s_{i,n_i} \left(\sum_{l=1}^{m_i} b_{i,l} \bar{u}_{i,l}^q + F_{i,n_i} + \Lambda_{i,n_i} - \dot{\alpha}_{i,n_i-1} + \breve{\varpi}_{i,n_i-1} \right) \le |s_{i,n_i}| \vartheta_{i,n_i} \tag{44}$$

In this step, the feasible virtual control signal α_{i,n_i} is designed as follows

$$\begin{aligned}\alpha_{i,n_i} = &\left(\frac{1}{2}+\frac{1}{2}\hat{\hbar}_{i,n_i}\bar{S}^{\mathrm{T}}_{m_{i,n_i}}\bar{S}_{m_{i,n_i}}\right)\mathrm{sign}(s_{i,n_i})K(\chi_{i,n_i})\\ &+\hat{\vartheta}_{i,n_i}\mathrm{sign}(s_{i,n_i})\left(1-K(\chi_{i,n_i})\right)+c_{i,n_i}s_{i,n_i}+s_{i,n_i-1}-\varpi_{i,n_i-1}\end{aligned} \tag{45}$$

The parameter adaptive laws $\dot{\hat{\hbar}}_{i,n_i}$ and $\dot{\hat{\vartheta}}_{i,n_i}$ are designed as follows

$$\dot{\hat{\hbar}}_{i,n_i} = \left(\frac{1}{2}\bar{S}^{\mathrm{T}}_{m_{i,n_i}}\bar{S}_{m_{i,n_i}}|s_{i,n_i}|-\hat{\hbar}_{i,n_i}\right)K(\chi_{i,n_i}) \tag{46}$$

$$\dot{\hat{\vartheta}}_{i,n_i} = \left(|s_{i,n_i}|-\hat{\vartheta}_{i,n_i}\right)\left(1-K(\chi_{i,n_i})\right) \tag{47}$$

where $c_{i,n_i}>0$ is a design parameter, and $\chi_{i,n_i}=[x_{i,1},x_{i,2},\ldots,x_{i,n_i}]^{\mathrm{T}}$.

Substituting (42), (44), (45), (46), and (47) into (40), we obtain

$$\begin{aligned}\dot{V}_{i,n_i} \le &-\sum_{\lambda=1}^{n_i}c_{i,\lambda}s_{i,\lambda}^2+\sum_{\lambda=1}^{n_i}\left|\tilde{\hbar}_{i,\lambda}\hat{\hbar}_{i,\lambda}\right|+\sum_{\lambda=1}^{n_i}\left|\tilde{\vartheta}_{i,\lambda}\hat{\vartheta}_{i,\lambda}\right|\\ &+s_{i,n_i}\sum_{l=1}^{m_i}b_{i,l}\rho_{i,l}^{q}(t)u_{i,cl}+s_{i,n}\alpha_{i,n_i}-\pi_i\tilde{\omega}_i\dot{\hat{\omega}}_i\end{aligned} \tag{48}$$

Then, design the actual controller $u_{i,cl}$ and the parameter adaptive law $\dot{\hat{\omega}}_i$ as follows

$$u_{i,cl} = -\mathrm{sign}(b_{i,l})\frac{s_{i,n_i}\hat{\omega}_i^2\alpha_{i,n_i}^2}{\sqrt{s_{i,n_i}^2\hat{\omega}_i^2\alpha_{i,n_i}^2+\sigma_i^2}} \tag{49}$$

$$\dot{\hat{\omega}}_i = \alpha_{i,n_i}s_{i,n_i}-\hat{\omega}_i \tag{50}$$

where σ_i is a smooth and bounded positive function.

Subsequently, substituting (49) and (50) into (48), we obtain

$$\dot{V}_{i,n_i} \le -\sum_{\lambda=1}^{n_i}c_{i,\lambda}s_{i,\lambda}^2+\sum_{\lambda=1}^{n_i}\left|\tilde{\hbar}_{i,\lambda}\hat{\hbar}_{i,\lambda}\right|+\sum_{\lambda=1}^{n_i}\left|\tilde{\vartheta}_{i,\lambda}\hat{\vartheta}_{i,\lambda}\right|+\pi_i\tilde{\omega}_i\hat{\omega}_i+\pi_i\sigma_i \tag{51}$$

3.3. Stability analysis

Theorem 1. *If the NMASs (1) with actuator failures (2) satisfies Assumptions 1–5, then the improved controllers (49), the parameter adaptive laws (24), (25), (35), (36), (46), (47), (50), the virtual control signals (23), (34), (45), can guarantee*

(1) All signals of the closed-loop system are GUUB.

(2) The consensus-tracking errors e_i can always be restricted within a specified range, i.e., $-\frac{\sqrt{\eta_i}}{\sqrt{\phi_i^2-1}}<e_i<\frac{\sqrt{\eta_i}}{\sqrt{\phi_i^2-1}}$.

(3) The consensus-tracking errors e_i converges to a prescribed range within a prescribed time T_s, i.e., when $t>T_s$, $-\frac{\sqrt{\eta_i}\gamma_i}{\sqrt{1-\gamma_i^2}}<e_i<\frac{\sqrt{\eta_i}\gamma_i}{\sqrt{1-\gamma_i^2}}$.

Proof. Treating the final Lyapunov function of NMASs (1) as follows

$$V=\sum_{i=1}^{N}V_{i,n_i} \tag{52}$$

Therefore, we can obtain from (51) that

$$\dot{V}\le\sum_{i=1}^{N}\left(-\sum_{\lambda=1}^{n_i}c_{i,\lambda}s_{i,\lambda}^2+\sum_{\lambda=1}^{n_i}\left|\tilde{\hbar}_{i,\lambda}\hat{\hbar}_{i,\lambda}\right|+\sum_{\lambda=1}^{n_i}\left|\tilde{\vartheta}_{i,\lambda}\hat{\vartheta}_{i,\lambda}\right|+\pi_i\tilde{\omega}_i\hat{\omega}_i+\pi_i\sigma_i\right) \tag{53}$$

According to Lemma 6 in [49], we can easily have

$$\sum_{\lambda=1}^{n_i}\left|\tilde{\hbar}_{i,\lambda}\hat{\hbar}_{i,\lambda}\right|\le\sum_{\lambda=1}^{n_i}\left|\hbar_{i,\lambda}^2-\tilde{\hbar}_{i,\lambda}^2\right|\le\sum_{\lambda=1}^{n_i}\hbar_{i,\lambda}^2 \tag{54}$$

$$\sum_{\lambda=1}^{n_i}\left|\tilde{\vartheta}_{i,\lambda}\hat{\vartheta}_{i,\lambda}\right|\le\sum_{\lambda=1}^{n_i}\left|\vartheta_{i,\lambda}^2-\tilde{\vartheta}_{i,\lambda}^2\right|\le\sum_{\lambda=1}^{n_i}\vartheta_{i,\lambda}^2 \tag{55}$$

$$\tilde{\omega}_i\hat{\omega}_i\le\omega_i^2-\tilde{\omega}_i^2\le\omega_i^2 \tag{56}$$

Substituting (54), (55), and (56) into (53), we obtain

$$\begin{aligned}\dot{V} &\le \sum_{i=1}^{N}\left(-\sum_{\lambda=1}^{n_i} c_{i,\lambda}s_{i,\lambda}^2 + \sum_{\lambda=1}^{n_i}\hbar_{i,\lambda}^2 + \sum_{\lambda=1}^{n_i}\vartheta_{i,\lambda}^2 + \pi_i\omega_i^2 + \pi_i\sigma_i\right)\\ &\le -\wp V + \Xi\end{aligned} \tag{57}$$

where $\Xi = \sum_{i=1}^{N}\left(\sum_{\lambda=1}^{n_i}\hbar_{i,\lambda}^2 + \sum_{\lambda=1}^{n_i}\vartheta_{i,\lambda}^2 + \pi_i\omega_i^2 + \pi_i\sigma_i\right)$, $\wp = \min\left\{2c_{i,\lambda}, 1\right\}$.

Integrating (57), we obtain

$$V(t) \le V(0)e^{-\wp t} + \frac{\Xi}{\wp}. \tag{58}$$

From (58), it can be seen that all signals of the closed-loop system are bounded. Since $s_{i,1}$ is bounded, z_i and $\Psi_i(e_i)$ are also bounded, and therefore e_i is bounded.

Based on the above analysis and recalling Remark 7, we initially conclude that $z_i(0) = \phi_i(0)\Psi_i(e(0)) = \Psi_i(e(0)) \in (-1, 1)$, which is bounded. Subsequently, since $s_{i,1}$ is bounded, it can be inferred that there exists a constant $\underline{k}_i$ such that

$$\left|z_i(t)\right| \le \underline{k}_i < 1, \forall t \ge 0 \tag{59}$$

Subsequently, according to (13), we have

$$-\emptyset_i(t) = -\frac{1}{\phi_i(t)} < -\frac{\underline{k}_i}{\phi_i(t)} \le \Psi_i(e_i) < \frac{\underline{k}_i}{\phi_i(t)} < \frac{1}{\phi_i(t)} = \emptyset_i(t) \tag{60}$$

Therefore, based on the properties of (10), we have

$$\psi_i(-\emptyset_i(t)) < \psi(\Psi_i(e_i)) < \psi_i(\emptyset_i(t)) \tag{61}$$

Since $\psi(\Psi_i(e_i)) = e_i$, so we have $\psi_i(-\emptyset_i(t)) < e_i < \psi_i(\emptyset_i(t))$. According to the analysis in Remark 4, we have

$$-\frac{\sqrt{\eta_i}}{\sqrt{\phi_i^2 - 1}} < e_i < \frac{\sqrt{\eta_i}}{\sqrt{\phi_i^2 - 1}} \tag{62}$$

$$-\frac{\sqrt{\eta_i}\gamma_i}{\sqrt{1-\gamma_i^2}} < e_i < \frac{\sqrt{\eta_i}\gamma_i}{\sqrt{1-\gamma_i^2}}, t \ge T_s \tag{63}$$

Finally, the proof of Theorem 1 is completed.

According to Lemma 2 in [50], we have

$$\left(y_i - y_d\right)^2 \le \|\bar{y} - \bar{y}_d\| \le \frac{\|\bar{e}\|}{\underline{\sigma}(\mathcal{L} + \mathcal{B})} \tag{64}$$

where $\bar{y} = [y_1, \ldots, y_N]^{\mathrm{T}}$, $\bar{y}_d = [y_d, \ldots, y_d]^{\mathrm{T}}$, $\bar{e} = [e_1, \ldots, e_N]^{\mathrm{T}}$. As per [51], $\underline{\sigma}(\mathcal{L} + \mathcal{B})$ possesses a conservative lower limit, determined by the number of agents N. Given the bounded nature of e_i, it can be inferred that the tracking error $y_i - y_d$ evolves within the predetermined range and converges to the specified region within the prescribed time.

Remark 10. Lemma 1 establishes that $(\mathcal{L} + \mathcal{B})$ is non-singular, serving exclusively for performance analysis and not for controller design. This aspect is pivotal in this paper, as it facilitates the development of a distributed controller that leverages local information among agents, ultimately ensuring global stability.

4. Simulation examples

In this section, we provide two practical examples to demonstrate the effectiveness of the proposed technique.

Example 1. In this example, three one-link robotic manipulators [25] are proposed as follows

$$\begin{cases} \dot{v}_i = \omega_i \\ J_i\dot{\omega}_i = \sum_{l=1}^{2} b_{i,l}u_{i,l} - M_i g l_i \sin(v_i) - h_{d_i}\omega_i \end{cases} \tag{65}$$

where $i = 1, 2, 3$. v_i and ω_i represent the angle and angular velocity, respectively. The parameters $l_i = \frac{2}{3}$m and $M_i = \frac{1}{3}$kg correspond to the length and mass of the pendulum for each agent. $g = 9.8$ m/s^2, $h_{d_i} = 0.2$, and $J_i = \frac{4}{3}M_i l_i^2$ are the gravitational acceleration, the friction coefficient, and the moment of inertia, respectively. The desired signal of the leader is given by $y_d(t) = \sin(t)$. Fig. 1 shows the leader–followers communication graph. From the figure, we can define that $\mathcal{L} = \begin{bmatrix} 0 & 0 & 0 \\ -1 & 1 & 0 \\ -1 & 0 & 1 \end{bmatrix}$. The faults model are as

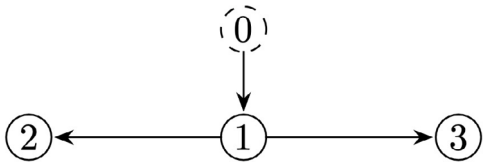

Fig. 1. Communication graph.

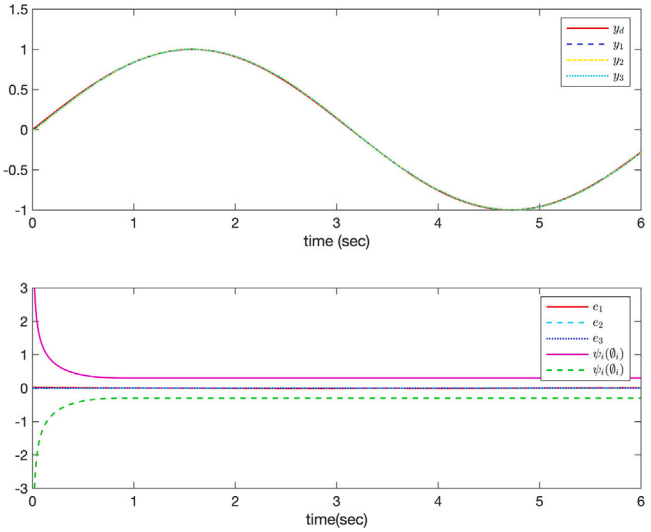

Fig. 2. The trajectories of system states and synchronization errors e_i.

follows

$$u_{i,1} = \begin{cases} 0.5u_{c,i1}, & \text{if } t \in [\check{j}T^*, (\check{j}+1)T^*) \\ u_{c,i1}, & \text{otherwise} \end{cases} \tag{66}$$

$$u_{i,2} = \begin{cases} 5 + 5\sin(5t), & \text{if } t \in [\check{j}T^*, (\check{j}+1)T^*) \\ u_{c,i2}, & \text{otherwise} \end{cases} \tag{67}$$

where $\check{j} = 1, 2, \ldots$, $T^* = 0.8$.

To accomplish the objective of this paper, the initial values are chosen as $\bar{\boldsymbol{x}}_{1,2}(\mathbf{0}) = [x_{1,1}(0), x_{1,2}(0)] = [0,0]^{\mathrm{T}}$, $\bar{\boldsymbol{x}}_{2,2}(\mathbf{0}) = [x_{2,1}(0), x_{2,2}(0)] = [0,0]^{\mathrm{T}}$, $\bar{\boldsymbol{x}}_{3,2}(\mathbf{0}) = [x_{3,1}(0), x_{3,2}(0)] = [0,0]^{\mathrm{T}}$. The proposed controller (49) is employed, along with the adaptive laws (35), (36), (46), (47), and (50), as well as the virtual control signals (34) and (45). Specifically, $T_s = 1$ and $\gamma_i = 0.3$ are selected. The control parameters employed in the proposed method are as follows: $c_{1,1} = 15$, $c_{1,2} = 10$, $c_{2,1} = 10$, $c_{2,2} = 12$, $c_{3,1} = 38$, $c_{3,2} = 80$, $n = 2$, $\check{a}_i = 2$, $\check{b}_i = 2$, $\iota_{i,11} = 0.45$, $\iota_{i,12} = 0.55$, $\iota_{i,21} = 0.85$, $\iota_{i,22} = 0.95$, $i = 1, 2, 3$.

The results of the simulation can be observed in Figs. 2–3. From Fig. 2, it can be seen that the output of the follower agents quickly tracks the reference signal of the leader agent, the consensus-tracking errors are always confined within the specified range and ensures that $|e_i| \leq 0.3$ when $t \geq 1$. Fig. 3 illustrate the trajectories of the inputs of the three agents.

Example 2. In this example, we consider a scenario with a virtual leader and three MSVs. The motion of the ith MSVs can be described by the kinematics in [26] as follows

$$\dot{\eta}_i = R_i\left(\bar{\psi}_i\right) \upsilon_i \tag{68}$$

and kinetics

$$M_i\dot{\upsilon}_i = u_i - C_{(\upsilon_i)}\upsilon_i - D_i(\upsilon_i)\upsilon_i + g_i\left(\eta_i, \upsilon_i\right) + d_i \tag{69}$$

where $\eta_i = [\bar{x}_i, \bar{\phi}_i, \bar{\psi}_i]^{\mathrm{T}} \in \mathbb{R}^3$ represents the position and yaw angle vector in earth coordinates, $\upsilon_i = [\bar{\omega}_i, \bar{v}_i, \bar{r}_i]^{\mathrm{T}}$ denotes the surge, sway, and yaw velocities in the body-fixed reference frame, and $u_i = [u_{\bar{\omega}_i}, u_{\bar{v}_i}, u_{\bar{r}_i}]^{\mathrm{T}} \in \mathbb{R}^3$ represents the control input. The term $g_i(\eta_i, \upsilon_i)$ represents the uncertain hydrodynamics, $M_i \in \mathbb{R}^{3\times3}$ is the inertia matrix, d_i denotes the unknown disturbance, and

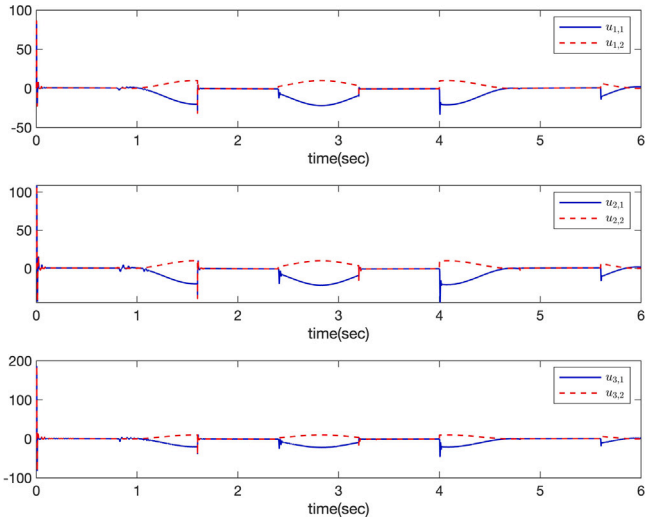

Fig. 3. The trajectories of $u_{1,1}$, $u_{1,2}$, $u_{2,1}$, $u_{2,2}$, $u_{3,1}$ and $u_{3,2}$.

$R_i(\bar{\psi}_i) \in \mathbb{R}^{3\times 3}$ is a rotation matrix given by

$$R_i(\bar{\psi}_i) = \begin{bmatrix} \cos(\bar{\psi}_i) & -\sin(\bar{\psi}_i) & 0 \\ \sin(\bar{\psi}_i) & \cos(\bar{\psi}_i) & 0 \\ 0 & 0 & 1 \end{bmatrix}.$$

When navigating, MSVs have motors that operate at high speeds for extended periods. Due to factors such as harsh marine environments, these motors are prone to frequent actuator failures, specifically intermittent actuator failures. Therefore, intermittent actuator failures are more common in MSVs. In this example, the actuator failure model is as follows

$$u_{i,1} = \begin{cases} (0.6 + 0.2\sin(0.5t))\, u_{c,i1}, & \text{if } t \in [\check{j}T^*, (\check{j}+1)T^*) \\ u_{c,i1}, & \text{otherwise} \end{cases} \tag{70}$$

$$u_{i,2} = \begin{cases} 8 + 4\cos(8t), & \text{if } t \in [\check{j}T^*, (\check{j}+1)T^*) \\ u_{c,i2}, & \text{otherwise} \end{cases} \tag{71}$$

where $\check{j} = 1, 2, \ldots$, $T^* = 0.8$. To achieve the control objectives of this paper, the selections of the communication topology graph, controllers, virtual controls, adaptive laws, and control parameters are the same as in Example 1. The difference is that the initial states are changed to $\bar{\boldsymbol{x}}_{1,2}(\mathbf{0}) = [x_{1,1}(0), x_{1,2}(0)]^{\mathrm{T}} = [1, 0]^{\mathrm{T}}$, $\bar{\boldsymbol{x}}_{2,2}(\mathbf{0}) = [x_{2,1}(0), x_{2,2}(0)]^{\mathrm{T}} = [2, 0]^{\mathrm{T}}$, and $\bar{\boldsymbol{x}}_{3,2}(\mathbf{0}) = [x_{3,1}(0), x_{3,2}(0)]^{\mathrm{T}} = [0, 0]^{\mathrm{T}}$.

The results of the simulation can be observed in Figs. 4–5. From Fig. 4, it can be seen that the output of the follower agents quickly tracks the reference signal of the leader agent, the consensus-tracking errors are always confined within the specified range and ensures that $|e_i| \leq 0.3$ when $t \geq 1$. Fig. 5 illustrate the trajectories of the inputs of the three agents.

5. Conclusion

This paper proposes a distributed adaptive FTC method for NMASs with actuator failures and prescribed performance. Firstly, time-varying scalar functions and normalization functions with prescribed settling time and tracking accuracy are given, and a barrier function is proposed on this basis to eliminate restrictions on initial conditions. Then, in order to address unknown nonlinear functions, a combination of MTN control and robust control techniques is utilized. A continuous switching function is devised to seamlessly transition from MTN control to robust control when the arguments of the unknown nonlinear function lie beyond the active range of MTN. Finally, the virtual control signals whose derivatives are approximated by a finite-time differentiator and the fault-tolerant controllers are designed. The proposed method ensures that all signals in the NMASs are GUUB, while keeping the consensus-tracking errors within a specified range and achieving the prescribed accuracy within a prescribed time. Additionally, simulation results validate the effectiveness and practicality of the proposed method.

Unknown nonlinear phenomena, such as model uncertainties [49] or additional disturbances [52], are also frequently present in control systems. Therefore, the focus of future research will be to design an adaptive output feedback control scheme for nonlinear multi-agent systems with intermittent actuator failures, combined with disturbance observer technology.

CRediT authorship contribution statement

Li-Ting Lu: Writing – original draft, Software, Methodology, Formal analysis. **Shan-Liang Zhu:** Writing – original draft, Formal analysis. **Dong-Mei Wang:** Methodology. **Yu-Qun Han:** Writing – review & editing, Software, Funding acquisition, Formal analysis.

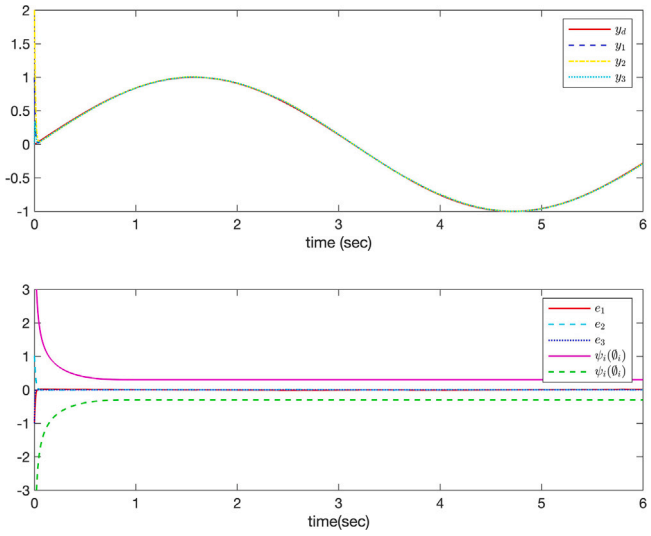

Fig. 4. The trajectories of system states and synchronization errors e_i.

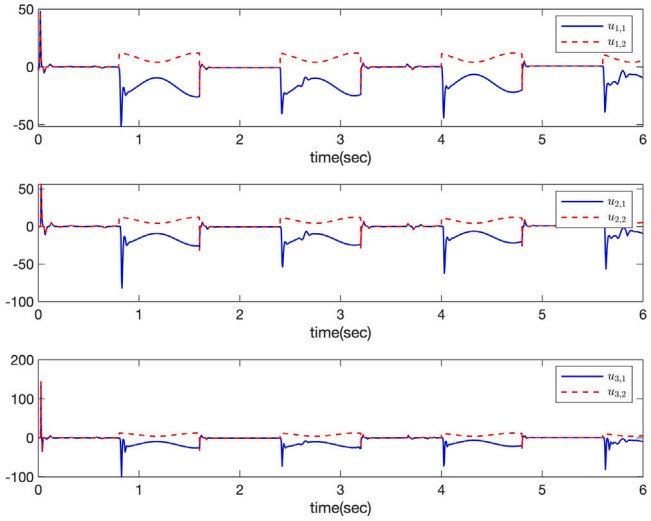

Fig. 5. The trajectories of $u_{1,1}$, $u_{1,2}$, $u_{2,1}$, $u_{2,2}$, $u_{3,1}$ and $u_{3,2}$.

Declaration of competing interest

The authors declare that they have no known competing financial interests or personal relationships that could have appeared to influence the work reported in this paper.

Data availability

No data was used for the research described in the article.

References

[1] Liang D, Dong Y. Robust cooperative output regulation of linear uncertain multi-agent systems by distributed event-triggered dynamic feedback control. Neurocomputing 2022;483:1–9.

[2] Chen C, Wen CY, Liu Z, Xie K, Zhang Y, Chen CP. Adaptive consensus of nonlinear multi-agent systems with non-identical partially unknown control directions and bounded modelling errors. IEEE Trans Autom Control 2017;62(9):4654–9.

[3] Deng C, Wen CY, Wang W, Li XY, Yue D. Distributed adaptive tracking control for high-order nonlinear multiagent systems over event-triggered communication. IEEE Trans Autom Control 2023;68(2):1176–83.

[4] Li ZX, Ji HB. Finite-time consensus and tracking control of a class of nonlinear multiagent systems. IEEE Trans Autom Control 2018;63(12):4413–20.
[5] Su HS, Wang XF, Yang W. Flocking in multi-agent systems with multiple virtual leaders. Asian J Control 2008;10(2):238–45.
[6] Dong XW, Hu GQ. Time-varying formation control for general linear multi-agent systems with switching directed topologies. Automatica 2016;73:47–55.
[7] Mu R, Wei AR, Li HT, Yue L. Leader-following consensus for multi-agent systems with actuator faults via adaptive event-triggered control. J Franklin Inst 2021;358(2):1327–49.
[8] Ni JK, Liu L, Tang Y, Liu CX. Predefined-time consensus tracking of second-order multiagent systems. IEEE Trans Syst, Man, Cybern: Syst 2021;51(4):2550–60.
[9] Ni JK, Wen CY, Zhao Y. Fixed-time leader-follower quantized output consensus of high-order multi-agent systems over digraph. Inform Sci 2022;587:408–34.
[10] Wang CL, Wen CY, Guo L. Adaptive consensus control for nonlinear multiagent systems with unknown control directions and time-varying actuator faults. IEEE Trans Autom Control 2021;66(9):4222–9.
[11] Wang W, Wen CY, Huang JS. Distributed adaptive asymptotically consensus tracking control of nonlinear multi-agent systems with unknown parameters and uncertain disturbances. Automatica 2017;77:133–42.
[12] Wu J, Sun W, Su SF, Xia JW. Neural-based adaptive control for nonlinear systems with quantized input and the output constraint. Appl Math Comput 2022;413:126637.
[13] Qin JH, Zhang GS, Zheng WX, Kang Y. Neural network-based adaptive consensus control for a class of nonaffine nonlinear multiagent systems with actuator faults. IEEE Trans Neural Netw Learn Syst 2019;30(12):3633–44.
[14] Ren HR, Liu ZY, Liang HJ, Li HY. Pinning-based neural control for multiagent systems with self-regulation intermediate event-triggered method. IEEE Trans Neural Netw Learn Syst 2024;1–11. http://dx.doi.org/10.1109/TNNLS.2024.3386881.
[15] Kang SJ, Liu PXP, Wang HQ. Command filter-based adaptive fuzzy decentralized control for stochastic nonlinear large-scale systems with saturation constraints and unknown disturbance. ISA Trans 2023;135:476–91.
[16] Jing YH, Yang GH. Fuzzy adaptive quantized fault-tolerant control of strict-feedback nonlinear systems with mismatched external disturbances. IEEE Trans Syst, Man, Cybern: Syst 2020;50(9):3424–34.
[17] Lin GH, Ren HR, Zhou Q, Wang XZ. Fuzzy dynamic event-triggered containment control for human-in-the-loop MASs with error constraints. IEEE Trans Fuzzy Syst 2024;32(4):2496–508.
[18] He WJ, Zhu SL, Li N, Han YQ. Adaptive finite-time control for switched nonlinear systems subject to multiple objective constraints via multi-dimensional Taylor network approach. ISA Trans 2023;136:323–33.
[19] He WJ, Zhu SL, Lu LT, Zhao W, Han YQ. Adaptive multi-switching-based global tracking control for switched nonlinear systems with prescribed performance. IEEE Trans Autom Sci Eng 2023;1–10. http://dx.doi.org/10.1109/TASE.2023.3277470.
[20] Wang MX, Zhu SL, Liu SM, Du Y, Han YQ. Design of adaptive finite-time fault-tolerant controller for stochastic nonlinear systems with multiple faults. IEEE Trans Autom Sci Eng 2023;20(4):2492–502.
[21] Wang Z, Shan JJ. Fixed-time consensus for uncertain multi-agent systems with actuator faults. J Franklin Inst 2020;357(2):1199–220.
[22] Sader M, Chen ZQ, Liu ZX, Deng C. Distributed robust fault-tolerant consensus control for a class of nonlinear multi-agent systems with intermittent communications. Appl Math Comput 2021;403:126166.
[23] Dong GW, Li HY, Ma H, Lu RQ. Finite-time consensus tracking neural network FTC of multi-agent systems. IEEE Trans Neural Netw Learn Syst 2021;32(2):653–62.
[24] Wang W, Wen CY. Adaptive compensation for infinite number of actuator failures or faults. Automatica 2011;47(10):2197–210.
[25] Wu W, Tong SC. Fuzzy adaptive consensus control for nonlinear multiagent systems with intermittent actuator faults. IEEE Trans Cybern 2023;53(5):2969–79.
[26] Wu W, Li YM, Tong SC. Neural network output-feedback consensus fault-tolerant control for nonlinear multiagent systems with intermittent actuator faults. IEEE Trans Neural Netw Learn Syst 2023;34(8):4728–40.
[27] Liu JH, Wang CL, Xu YJ. Distributed adaptive output consensus tracking for high-order nonlinear time-varying multi-agent systems with output constraints and actuator faults. J Franklin Inst 2020;357(2):1090–117.
[28] Li Y, Wang CL, Cai X, Li L, Wang G. Neural-network-based distributed adaptive asymptotically consensus tracking control for nonlinear multiagent systems with input quantization and actuator faults. Neurocomputing 2020;349:64–76.
[29] Chen WS, Ge SS, Wu J, Gong MG. Globally stable adaptive backstepping neural network control for uncertain strict-feedback systems with tracking accuracy known a priori. IEEE Trans Neural Netw Learn Syst 2015;26(9):1842–54.
[30] Wu J, Chen WS, Yang FZ, Li J, Zhu Q. Global adaptive neural control for strict-feedback time-delay systems with predefined output accuracy. Inform Sci 2015;301:27–43.
[31] Wu J, Chen WS, Zhao D, Li J. Globally stable direct adaptive backstepping NN control for uncertain nonlinear strict-feedback systems. Neurocomputing 2013;122:134–47.
[32] Wu J, Su BY, Li J, Zhang X, Ai L. Global adaptive neural tracking control of nonlinear MIMO systems. Neural Comput Appl 2017;28:3801–13.
[33] Ni JK, Shi P. Global predefined time and accuracy adaptive neural network control for uncertain strict-feedback systems with output constraint and dead zone. IEEE Trans Syst, Man, Cybern: Syst 2021;51(12):7903–18.
[34] Bechlioulis CP, Rovithakis GA. Robust adaptive control of feedback linearizable MIMO nonlinear systems with prescribed performance. IEEE Trans Autom Control 2008;53(9):2090–9.
[35] Wang W, Ma H, Basin MV, Liang HJ. Adaptive event-triggered consensus control of multi-agent systems with prescribed performance and input quantization. Internat J Adapt Control Signal Process 2021;35(8):1454–77.
[36] Wang W, Liang HJ, Pan YN, Li TS. Prescribed performance adaptive fuzzy containment control for nonlinear multiagent systems using disturbance observer. IEEE Trans Cybern 2020;50(9):3879–91.
[37] Liu JH, Wang CL, Cai X. Adaptive neural network finite-time tracking control for a class of high-order nonlinear multi-agent systems with powers of positive odd rational numbers and prescribed performance. Neurocomputing 2021;419:157–67.
[38] Zhao K, Song YD, Chen CP, Chen L. Adaptive asymptotic tracking with global performance for nonlinear systems with unknown control directions. IEEE Trans Autom Control 2022;67(3):1566–73.
[39] Lin ZB, Liu Z, Su CY, Wang YN, Chen CP, Zhang Y. Adaptive fuzzy prescribed performance output-feedback cooperative control for uncertain nonlinear multiagent systems. IEEE Trans Fuzzy Syst 2023;31(12):4459–70.
[40] Huang CJ, Liu Z, Chen CP, Zhang Y. Adaptive fixed-time neural control for uncertain nonlinear multiagent systems. IEEE Trans Neural Netw Learn Syst 2023;34(12):10346–58.
[41] Liu Y, Yao DY, Wang LJ, Lu SJ. Distributed adaptive fixed-time robust platoon control for fully heterogeneous vehicles. IEEE Trans Syst, Man Cybern: Syst 2023;53(1):264–74.
[42] Liu Y, Li HY, Lu RQ, Zuo ZY, Li XD. An overview of finite/fixed-time control and its application in engineering systems. IEEE/CAA J Autom Sin 2022;9(12):2106–20.
[43] Boskovic J, Mehra R. Stable multiple model adaptive flight control for accommodation of a large class of control effector failures. In: Proceedings of the 1999 American control conference (cat. no. 99CH36251), vol. 3, 1999, p. 1920–4.
[44] Zhu JY, Shen QK, Zhang TP, Yi Y. Decentralized finite-time adaptive neural FTC with unknown powers and input constraints. Inform Sci 2024;656:119909.

[45] Shen QK, Shi P, Lim CP. Fuzzy adaptive fault-tolerant stability control against novel actuator faults and its application to mechanical systems. IEEE Trans Fuzzy Syst 2024;32(4):2331–40.
[46] Shen QK, Yi Y, Zhang TP. Fuzzy adaptive distributed synchronization control of uncertain multi-agents systems with unknown input power and sector nonlinearities. Chaos Solitons Fractals 2023;174:113897.
[47] Spooner JT, Maggiore M, Ordonez R, Passino KM. Stable Adaptive Control and Estimation for Nonlinear Systems: Neural and Fuzzy Approximator Techniques. John Wiley & Sons; 2004.
[48] Wang WR, Tan F, Ge HL, Wu JX, Zhang Y. Adaptive integral backstepping control of PMSM with differential terms based on parameters fuzzy self-tuning. Int J Innovative Comput Inf Control 2019;15(6):2165–81.
[49] Ren HR, Ma H, Li HY, Wang ZY. Adaptive fixed-time control of nonlinear MASs with actuator faults. IEEE/CAA J Autom Sin 2023;10(5):1252–62.
[50] Shang Y, Chen B, Lin C. Consensus tracking control for distributed nonlinear multiagent systems via adaptive neural backstepping approach. IEEE Trans Syst, Man, Cybern: Syst 2020;50(7):2436–44.
[51] Bechlioulis CP, Rovithakis GA. Decentralized robust synchronization of unknown high order nonlinear multi-agent systems with prescribed transient and steady state performance. IEEE Trans Autom Control 2017;62(1):123–34.
[52] Ren HR, Ma H, Li HY, Lu RQ. A disturbance observer based intelligent control for nonstrict-feedback nonlinear systems. Sci China Technol Sci 2023;66(2):456–67.